IEEE Access
Multidisciplinary | Rapid Review | Open Access Journal

Received 19 February 2024, accepted 26 February 2024, date of publication 29 February 2024, date of current version 6 March 2024.

Digital Object Identifier 10.1109/ACCESS.2024.3371906

RESEARCH ARTICLE

Future 6G Communications Powering Vertical Handover in Non-Terrestrial Networks

ANIRUDH WARRIER[1], LAMEES ALJABURI[2], HUW WHITWORTH[1], SABA AL-RUBAYE[1], (Life Senior Member, IEEE), AND ANTONIOS TSOURDOS[1]

[1]Centre for Autonomous and Cyberphysical Systems, Cranfield University, MK43 0AL Bedford, U.K.
[2]Department of Computer Engineering, Faculty of Engineering, Near East University, Nicosia 99138, Cyprus

Corresponding author: Anirudh Warrier (anirudh.warrier@cranfield.ac.uk)

This work was supported by the Engineering and Physical Sciences Research Council (EPSRC) and Satellite Applications Catapult.

ABSTRACT The integration of Unmanned Aerial Vehicles (UAVs) into future 6G networks will open new possibilities for applications ranging from surveillance to communication infrastructure maintenance, precision agriculture, and surveying. However, ensuring uninterrupted connectivity for UAVs operating in remote or dynamic environments remains a significant challenge. This paper presents a novel approach to achieving seamless handover for UAVs when transitioning between terrestrial and satellite communication networks. The proposed method in this paper, leverages graph theory and develop a decision-making algorithm to optimise handover decisions, minimizing latency, improving performance, and reducing service disruption. It establishes a comprehensive graph model that represents the dynamic topology of available network nodes, including terrestrial base stations and low earth orbit (LEO) satellites, which adapts in real-time to changes in UAV position and network conditions. The approach incorporates a decision-making algorithm that considers several factors, such as received signal strength (RSS), signal-to-noise ratio (SNR), and elevation angle, to determine the optimal time and location for a handover between terrestrial base stations and satellite links. This ensures a seamless transition between communication links, minimizing service disruption. The performance of this method is evaluated through extensive simulations and comparison with existing solutions demonstrating significant improvements in RSS, SNR, throughput, latency, ping-pongs and enhanced overall UAV connectivity. The proposed graph method-based seamless handover solution represents a crucial advancement in enabling reliable and uninterrupted communication for UAVs operating in remote and challenging environments. By managing handovers between terrestrial and satellite networks, this research contributes to the realisation of the full potential of UAVs in emerging applications, thereby advancing the state-of-the-art in UAV technology.

INDEX TERMS 6G, vertical handover, satellite, graph method, non-terrestrial networks (NTN).

I. INTRODUCTION

The development of telecommunication networks towards the Sixth Generation of Mobile Communications (6G) entails a significant transformation in the infrastructure and technologies employed. 6G can support a greater number of users and devices with diverse performance requirements, as well as an increased number of applications and use cases. The traditional terrestrial mobile network is limited in its ability to provide coverage in certain areas, such as remote, non-land regions, and disaster-stricken areas due to infrastructure limitations.

The utilization of Non-Terrestrial Networks (NTNs) in conjunction with the future 6G networks presents a viable and economically efficient approach to ensuring uninterrupted and pervasive wireless coverage, consequently facilitating network scalability [1]. In these scenarios, NTNs function as access nodes that enhance the capabilities of the existing terrestrial networks, encompassing aspects such as capacity, coverage, and latency. Furthermore, this approach holds the

The associate editor coordinating the review of this manuscript and approving it for publication was Barbara Masini.

© 2024 The Authors. This work is licensed under a Creative Commons Attribution 4.0 License.
For more information, see https://creativecommons.org/licenses/by/4.0/

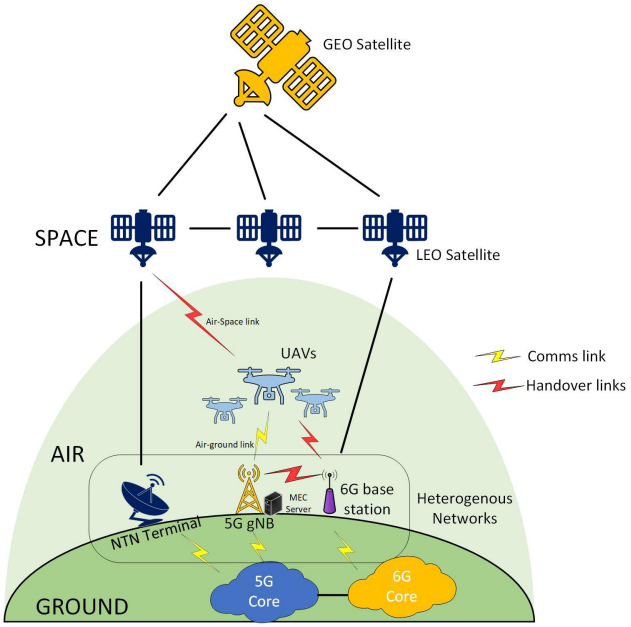

FIGURE 1. Integrated vertical heterogeneous networks.

potential to mitigate the deficiencies inherent in terrestrial infrastructure, enabling it to meet the requisite standards of reliability and widespread accessibility for forthcoming wireless applications.

Satellites present a viable solution as they are not constrained by geographical environments, offering the potential for global coverage. Geostationary Earth Orbit (GEO) satellites, positioned at an altitude of 35,786 km above the equator and moving synchronously with the Earth, cover nearly one-third of the Earth's surface. However, the inherent propagation delay associated with GEO satellites may fall short of meeting the stringent requirements of delay-sensitive services. Conversely, Low Earth Orbit (LEO) satellites, situated at altitudes ranging from 300 to 1500 km, undergo frequent handovers (HOs) due to their rapid orbital movement. Moreover, LEO satellites exhibit limited coverage areas, and in instances where the constellation size is modest, specific regions may remain unattended. Despite these challenges, the emerging era of integrated vertical heterogeneous networks, as proposed in [2], anticipates a pivotal role for LEO satellites in delivering global communication and internet services.

In figure 1 such a network is shown, where there are three layers of network. the first one is the ground segment where the terrestrial network components namely the base stations, the respective core network, and the Multi-Access Edge Computing (MEC) architecture. The second segment is the air segment, which consists of the flying vehicles or Unmanned Aerial vehicles (UAVs). Finally, the third segment is the space segment, which has two levels, firstly the LEO satellites which are deployed as constellations and the second level which consists of GEO satellites.

To achieve a vertical seamless HO for a network as shown in figure 1, efficient techniques and algorithms must be devised. As detailed in further sections, reliable solutions exist for ground based vertical HO for UAVs [3], [4], [5]. However, air-to-space remains unexplored for UAV networks.

Commercial companies like SpaceX and Amazon have launched segments of LEO satellite constellations that guarantees worldwide connectivity [6]. Compared to GEO satellites, LEO satellites have lower propagation delays, require less transmission power, and suffer from reduced signalling attenuation. This allows for direct communication with UAVs to be established easily. The primary objective of these satellite systems is to augment and extend the current terrestrial networks, ensuring comprehensive global coverage. These systems have the capacity to collaborate with established fixed networks, facilitating the sharing of instantaneous traffic loads. Broadly speaking, satellite networks serve to expand coverage to areas where the deployment of terrestrial wireless systems is impractical, either due to economic constraints or geographical limitations. The system model is shown in figure 2 and the highlighted part represents a rural area where terrestrial systems become infeasible. This is the primary focus of this work.

The aim of this paper is to seamlessly integrate terrestrial networks with satellite networks for the reliable and safe operation of UAVs. To this aim, a novel graph method-based HO decision algorithm is proposed in this paper. The system is modelled as a graph, with the terrestrial base stations and satellites acting as the nodes, while the decision criteria (signal parameters in this case) acting as the edges.

The paper presents existing work through an extensive literature survey, as 6G is not yet standardized, we consider similar works within legacy technologies and highlight the research gaps in Section II. It also presents the novel contributions of this work. Based on this survey, the air-air HO challenge is identified and described in Section III. In Section IV, the graph-based decision-making algorithm is described, along with its implementation using weighted summation model (WSM), and Dijkstra's algorithm. The system model, network model and the channel model used in this work is described in section V, along with the simulation setup. Additionally, the results visualized in different plots are discussed in this section. Finally, the impact of the results is discussed, and future directions are described in the conclusion section VI.

II. BACKGROUND AND RELATED WORKS

In recent years, there has been a surge of interest among various companies in providing widespread internet connectivity from space. This renewed focus gained momentum following the successful implementation of projects such as Starlink and OneWeb [7], [8].

The 3rd Generation Partnership Project (3GPP) conducted comprehensive studies aimed at delineating the potential role of NTNs within the fifth-generation (5G) ecosystem

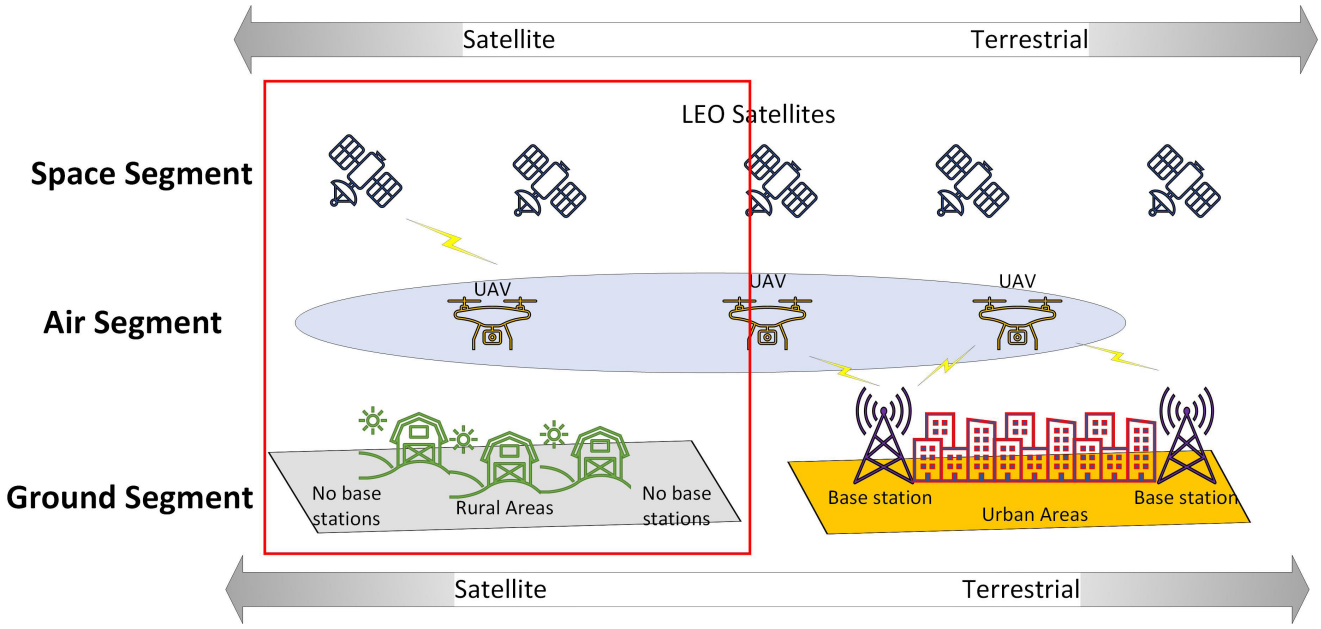

FIGURE 2. Satellite connectivity in rural areas.

during Release 15 [9]. Subsequently, in Release 16 [10] the 3GPP is proffering networking solutions to facilitate the seamless integration of non-terrestrial (NT) and terrestrial networks. A distinguishing feature among these proposed solutions lies in the allocation of functionalities on NT objects. These objects may serve as relay nodes, connecting 5G User Equipment (UE) and the 5G access point, thereby extending the 5G Radio Access Network (RAN) coverage. Alternatively, they can function as a backbone support. Furthermore, an additional study explored the potential utilization of Satellite Communication (SatCom) networks as active nodes in 5G access operations, effectively generating 5G cells akin to 5G Next generation Node B (gNB) [11]. Several ongoing research projects are diligently investigating the role of satellites and UAVs within the 5G framework, with the intent of developing and testing solutions for future implementation within the 5G network. For instance, the work presented in [12] sheds light on the outcomes of the ongoing SAT5G project, which is funded by the European Commission. The project focuses on satellite communications positioning within 5G scenarios, particularly geared toward enhancing Mobile Broadband (eMBB) capabilities. The overarching objective is to provide cost-effective, plug-and-play SatCom solutions while expediting 5G deployment across diverse geographical regions. The project has identified four distinct satellite use cases for eMBB, concentrating on efficient multicast/broadcast content delivery to network peripheries, augmenting terrestrial connectivity by providing 5G access to premises, extending 5G connectivity to mobile platforms such as airplanes, and provisioning 5G as a fixed backhaul in regions where deploying terrestrial connections is challenging, such as lakes and islands, among others.

Additionally, the work in [13] introduces a 5G-centric network architecture predicated on satellite communication and MEC. This architecture is designed to bolster eMBB applications and ensure an optimal Quality of Experience (QoE), particularly for live streaming applications. The evaluation of this approach was conducted using a real satellite link. A recently launched European Union (EU) project, ‘‘5G! Drones’’ [14], is dedicated to integrating UAVs into the 5G landscape. The authors designed, implemented, and conducted various UAV use cases integrating with 5G, while validating critical 5G Key Performance Indicators (KPIs). The envisaged use cases encompass UAV traffic management, public safety, life-saving operations, situational awareness, and providing connectivity during densely attended events.

These studies provide useful background into the landscape of UAVs, satellites and 5G and provide a foundation in future directions. This, however, does not discuss specifically the solution to the challenge of HO between terrestrial networks and satellites.

Another method to integrate terrestrial and NTNs is discussed in [15], where a concept of relay nodes (RN) is presented. This facilitates the transportation of 5G downlink/uplink waveforms via a LEO satellite link to the designated base station or the ground earth station. From the perspective of the onboard equipment, whether it be the flight controller necessitating Cell-Network Plane Communication (CNPC) or payload equipment requiring a high-throughput link, the RN functions akin to a conventional ground station. In scenarios where multiple UAVs are deployed as a swarm, the UAV equipped with the satellite-enabled RN can effectively serve as a ‘‘cell tower’’ for the entire fleet. For the

ground base station, which perceives the RN as transparent, it merely interacts with a group of users.

While this approach may not necessarily optimize channel capacity, it offers the advantage of reduced communication infrastructure requirements both on the UAV and ground station. It also does not deal with the HO problem.

Reference [16], presents an extensive survey on UAVs in 6G networks. UAVs, when harnessed in conjunction with 6G communication services, exhibit immense utility across a diverse spectrum of civic and commercial applications. The integration of 6G communication services empowers smart automation and the seamless assimilation of Artificial Intelligence (AI), thereby ushering in a new era characterized by innovative services, including ultra-smart cities, the Internet of Everything (IoE), Extended Reality (XR) encompassing Mixed Reality (MR), Virtual Reality (VR), and Augmented Reality (AR). Autonomous connectivity such as Wireless Brain-Computer Interaction (WBCI), autonomous vehicles, and AI-driven services. The anticipated capabilities of 6G communication networks promise to deliver a wireless connectivity enhancement of up to 100-fold and significant performance amplification compared to its predecessor, 5G. The primary drivers of 6G advancements encompass satellite connectivity, drones, connected intelligence supplemented by wireless power transfer, utilization of the terahertz (THz) band, Optical Wireless Communication (OWC), machine learning, and the development of three-dimensional (3D) networking [17], [18].

In the context of aerial communications, 6G introduces solutions that surmount several limitations inherent to prior generations of wireless communication technologies [19], [20], [21], [22]. The core attribute of 6G communication lies in its fusion of NTNs with 3D connectivity, seamlessly integrated with ubiquitous AI-based services within the 3D spatial domain, rendering it particularly well-suited for aerial communications [23]. 6G technologies promise to deliver uninterrupted connectivity, precision positioning capabilities, ultra-high bandwidth, and real-time remote-control functionalities tailored for high-density aerial vehicle environments. While THz bands may pose challenges for drone operations due to elevated path loss and constrained coverage, their integration with satellite networks presents a viable solution to address these issues [24], [25], [26], [27].

In a specific research endeavour presented in [28], the authors introduced an inter-satellite HO strategy grounded in potential game theory. The objective was to minimize the average number of HO events and evenly distribute the load within the satellite constellation network. However, it did not consider a terrestrial network and HO from such a network. Addressing the critical issues of HO delay and signalling cost reduction, [29] proposed various HO procedures designed for a multi-layer network architecture encompassing GEO satellites, high altitude platform systems (HAPS), and terrestrial relay nodes. The use of GEO satellites reduces the number of satellites required for connectivity, but it has challenges relating to high latency and higher signal attenuation. Reference [30] outlined a user-centric HO scheme tailored for ultra-dense LEO satellite networks. Their solution involved buffering user's downlink data across multiple satellites simultaneously, facilitating seamless HOs and mitigating the frequent HO issue. Reference [31] introduced a reinforcement learning scheme wherein UE autonomously made decisions to optimize long-term throughput while minimizing unnecessary HO events among NT base stations. This work does not consider HO for UAVs instead does it for UEs. Like conventional terrestrial wireless networks [32], NTNs can involve a NT Base Station (NT-BS) serving UEs. However, a fundamental distinction exists between NTNs and terrestrial wireless networks. In terrestrial wireless networks, Base Stations (BSs) are typically stationed at fixed locations without mobility. Consequently, multiple BSs can easily coordinate with each other to support seamless services and optimize mobility management through a network-driven user access control approach. Conversely, NTNs introduce a challenge due to the mobility of NT-BSs, including satellites orbiting the Earth travelling over significant distances. These NT-BSs exhibit high-speed mobility [33],with satellite speeds reaching up to 7,000 m/s. These rapid and continuous movements can disrupt the availability of links between NT-BSs, making it exceedingly difficult for them to directly coordinate with each other. Consequently, in NTNs, a UE-driven user access control scheme, where each UE autonomously selects an appropriate NT-BS, becomes a viable solution to address this challenge. While network-driven user access control schemes have demonstrated superior performance in terrestrial networks, there have been discussions on the development of UE-driven access control schemes in terrestrial networks. These UE-driven schemes often focus on the Received Signal Strength (RSS)-based method [34], [35] where UEs typically connect to the BS with the strongest RSS. The work done in the realm of HAPs HO, also proves to be a critical point of advancement. HAPs can be considered to have similar characteristics to that of a UAV and therefore HO strategies developed for HAPs, can be adopted for use within UAVs with certain modifications. Reference [36] proposes an adaptive hysteresis margin for HO within a Long Term Evolution (LTE) network, specifically attempting to reduce ping-pongs. The hysteresis margin relies on RSS measurements between the target and serving base stations. Its accurate determination, among other benefits, addresses the issue of excessive and repetitive handovers, commonly known as the ping-pong effect. The model proposed in this study incorporates the artificial neural network (ANN) mechanism into the determination of the hysteresis margin within the LTE handover process. This integration aims to minimize handover delay and mitigate ping-pong effects, accounting for the velocity of the UE. This method is effective in reducing ping-pongs for ground users but not for UAVs. Reference [37] proposes a design with different HO procedures suitable for LEO-HAP system

based on 5G protocol and analyse the performance on delay and signalling cost. They employ a dynamic HO strategy to optimize the HO moment and resource allocation. Lagrange duality is used, and a sub-gradient algorithm is presented. A prediction-based HO decision algorithm with an adaptive threshold is presented in [38]. An auto-regressive integrated moving average model (ARIMA) algorithm is proposed, that predicts the values of RSS using time series analysis model and dynamically adjust the HO initiation time according to the prediction. This proves to be an effective method, but as with other works, they cannot be implemented for UAVs. Even though, HAPs are like UAVs, they do have some fundamental differences that changes the pattern of HO algorithms. Firstly, HAPs are typically deployed at exceptionally high altitudes, often within the stratosphere. This elevated positioning affords a clear line of sight to extensive areas, minimizing obstacles and reducing signal blockages. Consequently, the channel can be modelled with relatively low path loss, rendering it well-suited for establishing long-range communication links. In contrast, UAVs operate at lower altitudes, and their line of sight may encounter obstructions such as buildings and terrain. Channel modelling for UAVs must therefore account for potential signal blockages, leading to increased path loss when compared to HAPs. Secondly, the development of a handover scheme involves managing the transition of communication links between base stations. In the realm of airborne platforms like UAVs and HAPs, the development of handover schemes may vary due to disparities in their characteristics and operational environments. HAPs are engineered to maintain a stationary or quasi-stationary position for extended durations, resulting in relatively predictable mobility characteristics. The associated mobility model may incorporate considerations for sustaining connectivity within a fixed coverage area. Conversely, UAVs are highly mobile platforms capable of rapid position changes. The mobility modelling for UAVs must adapt to the dynamic nature of their movement, encompassing scenarios involving handovers between ground stations and satellites. For UAVs, high mobility necessitates adaptive handover schemes to accommodate the UAV's changing location, ensuring seamless communication. Potential interference and obstacles in the communication path mandate mechanisms within the handover scheme to assess the QoS and mitigate interference or obstacles. Variability in communication range, influenced by factors like altitude, terrain, and interference, underscores the need for dynamically adjusting handover thresholds in real-time conditions [39], [40]. Table 1 summarises the existing works.

A. CONTRIBUTIONS

In this paper, a novel graph-based HO algorithm is proposed. The decision-making is performed as part of a time-based directed weighted graph, such that the satellites and base stations form the vertices and the signal parameters as edges. This paper therefore makes the following contributions:

- A heterogeneous satellite-ground networks is established to ensure UAVs can access either satellites or base stations seamlessly. UAVs can make these HO decisions independently.
- The decision functions are designed to reflect the signal parameters, viz. RSS, Signal-to-Noise-Ratio (SNR) and elevation angle. This is multi-criteria decision-making problem implemented through the WSM
- A graph theory-based algorithm is proposed, that implements the Dijkstra's algorithm for HO execution.

III. HANDOVER CHALLENGE IN AIR-TO-AIR NETWORKS

HO technology, is essential for maintaining uninterrupted connections during user transitions between cells. It is influenced by factors like signal level reduction, load balancing, and high error rates. UAVs, due to their unique characteristics, present specific challenges for effective HO management in mobile networks. These challenges include increased system complexity, the potential for Line-of-Sight (LoS) control, and higher HO rates due to UAV speed [45]. The primary differences between our previous work and this work has been highlighted in Table 2. Moreover, UAVs often rely on terrestrial antenna side-lobes, leading to frequent HOs, thereby degrading Quality of Service (QoS) [46].

Managing UAV HOs necessitates a distinct approach compared to conventional UE HO techniques. Techniques designed for terrestrial UEs may not be directly applicable to UAV networks due to the unique aspects of UAV operations. The primary goal is to ensure high-quality, reliable communication while facilitating seamless HOs among UAVs.

Although prior research has made efforts to address these challenges, substantial hurdles remain. For instance, we previously explored vertical HOs in urban environments [47], whereas this paper focuses on UAV HOs in rural areas with limited terrestrial infrastructure. In this scenario, UAVs transition between urban and rural regions, connecting to a LEO satellite when terrestrial infrastructure is lacking/absent. A graph-based decision-making HO algorithm, treating satellites and terrestrial base stations as vertices and using weighted summation models as edges for decision-making. HOs are executed within this framework through Dijkstra's shortest path algorithm.

The results indicate that the proposed algorithm outperforms existing solutions for similar networks, such as the adaptive threshold method and hysteresis method [43], and [38]. This research contributes to the advancement of effective HO management for UAVs operating in challenging, dynamic environments, enhancing the performance and reliability.

IV. GRAPH METHOD BASED HANDOVER DECISION ALGORITHM

A. GRAPH THEORY

In the rapidly evolving landscape of UAVs and NT satellite connectivity, ensuring seamless HOs between different

TABLE 1. Summary of literature survey.

Ref.	Problem formulation	Technology	Decision Criteria	Gap
[28]	HO strategy based on game theory	N/A	Terminal Random Access Maximization	When the number of users in game theory increases, it is challenging to implement.
[36]	HO with a hysteresis margin	Adaptive hysteresis method	ANN-based prediction	The method uses ANN for prediction and implementing the adaptation, which is computationally intensive and requires complex hyper-parameter tuning and requirements of large datasets for training. Additionally, this method has also been used for ground-based users and not UAVs
[38]	Monte Carlo Model	RSS-threshold algorithm combined with the ARIMA	Adaptive threshold	This is primarily implemented for HAPS, which is like UAVs. However, UAVs have different characteristics than HAPS.
[41]	HO as a Resource Allocation problem	Deep Reinforcement Learning	Markov Decision Process	It conducts network selection by allocating resources in multi-Radio Access Technology (RAT) network scenario. Although multi-RAT HO is of interest, this paper does not consider HO at the signal level. Furthermore, only accounts for ground UEs and no UAVs
[42]	HO based on Antenna Gain manipulation	Network-controlled HO	Gain value based, network controlled	This paper compares state of art HO mechanisms for UE-LEO satellites. It proposes a new method for intra-satellite HO, but no methods were discussed for UAVs or in a heterogeneous network environment.
[43]	HO based on QoS utility function optimization	Importance-Technique for Order of Preference by Similarity to Ideal Solution (TOPSIS)	Multi Attribute Decision Making (MADM)	It proposes a two-step, hybrid LEO-GEO satellite network. The system is, however, robust, which might not be suitable for the HO problem. Additionally, it does not consider UAV networks
[44]	HO based on QoS utility function optimization	Graph Theory	MADM	Inter-satellite HO is discussed in this paper using graph method. It does not include base station to satellite HO, only between satellites.
Proposed	HO based on WSM	Time-based graph theory	MADM	This paper introduces a novel approach utilizing graph theory algorithm to ensure uninterrupted connectivity for terrestrially connected UAVs during transitions between terrestrial and satellite networks. The method minimizes latency, ping-pongs, and service disruption, while increasing RSS, SNR and throughput. enhancing the reliability of UAV communication in remote and dynamic environments.

TABLE 2. Comparison with our previous work [45].

Work	Technologies used	Type of connectivity	Infrastructure scenario	Proposed Solution
[45]	LTE, 5G	Air-to-ground	Urban- base stations present	Entropy weighted method
Proposed	6G, Satellite	Air-to-air	Rural- base stations absent	graph based method

communication nodes is paramount. This paper introduces a novel approach, the graph method based seamless HO, designed to address the unique challenges of UAVs operating within terrestrial-satellite networks. This approach offers several key features that enhance the efficiency, reliability, and performance of UAV communication in dynamic, multi-node environments.

The foundation of this method lies in graph theory, where communication nodes, UAVs, and satellites are represented as nodes in a dynamic network graph. Edges between nodes represent decision making parameters. This model provides a comprehensive view of network topology, aiding in efficient HO decision-making. The graph-based approach enables proactive HO decisions by analysing signal RSS, SNR, elevation angle to ensure uninterrupted data transmission. By constantly evaluating available paths and selecting the most suitable ones, it ensures UAVs maintain a robust and consistent connection, even in challenging environments. The graph-based approach can scale to accommodate a growing number of UAVs and communication nodes, making it adaptable for various deployment scenarios.

B. PROBLEM FORMULATION

Firstly, the list of notations are presented in Table 3.

The problem is formulated as a graph with distinct instances of satellites and base stations denoted as s_1, s_2, s_3 and s_4 across a time duration T, segmented into several short, equidistant time intervals $t_1, t_2, \ldots, t_i$. The optimal time for HO from base station b_1 to any of the target satellites

TABLE 3. List of notations.

List of notations	Definition
T	Total time period of simulation
$s_1, s_2 ... s_q$	satellite instances
$BS_1, BS_2, ..BS_m$	Base station instances
δ	Relaxation Period
x_{gNB}	Signal Parameter for base station
$x_{satellite}$	Signal Parameter for satellite
M	Decision Matrix
G	Graph
V	Vertices
E	Edges
W	Weight matrix
$P_{i,m}$	received power
$\overline{P_{i,m}}$	Mean Power
Π_0	Free space pathloss
σ^2	Variance of shadowing
P_s	Signal power
P_N	Noise Power
s(t)	signal
$R_n(t)$	Correlation function for noise
$\|E[\cdot]\|$	Expected value
Δ	Delta Dirac function
v_{ij}	normalized matrix
K	Ratio of Power between direct and scattered paths
u^2	power from direct paths
$2\beta^2$	power from scattered paths
Ω	Total power from direct and scattered paths
A(d)	Atmospheric fading
χ	Attenuation through clouds and rain
d	Propagation distance
h	UAV altitude
(o_x, o_y)	position right to below the satellite
G	channel model
c	speed of light
f_c	Frequency
φ	Probability distribution function

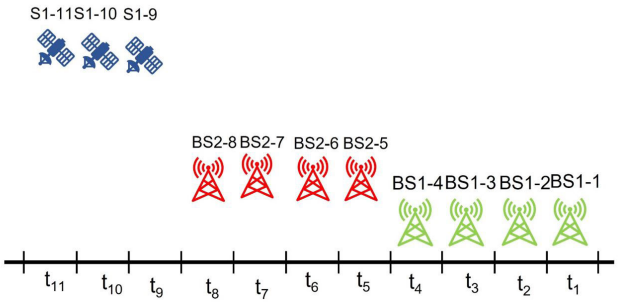

FIGURE 3. gNBs and satellites as time instances.

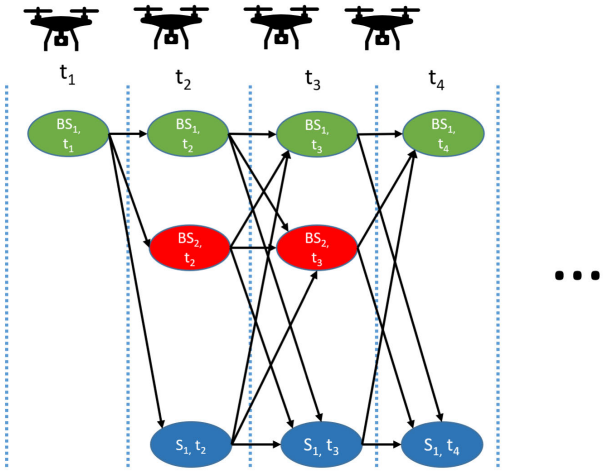

FIGURE 4. Representative graph for proposed model.

s_1, s_2, s_3 or s_4 is subject to various time-variable criteria. In the proposed framework, each satellite and base station is represented by multiple instances to account for changes in satellite communication status over time. For instance, in figure 3 the notations of the base stations and satellites with respect to the time are shown. This means that base stations BS_{1-1}, BS_{1-2}, BS_{1-3}, BS_{1-4} represent the base stations at time duration t_1, t_2, t_3 and t_4. Similarly for base stations at time duration t_5, t_6, t_7, and t_8. In the case of satellites, they are represented at time duration t_9, t_{10} and t_{11} as s_{1-9}, s_{1-10} and s_{1-11}. Given the context of the Starlink satellite network with numerous LEO satellites and overlapping coverage periods, the GPS-based approach outlined in [48] and the simplified general perturbations (SGP4) model from [49] are employed to determine UAV positions and LEO satellite information.

Consider a scenario where, for a given UAV, a sequence of HOs is necessary from a base station to a satellite over a time duration T. As previously mentioned, T is divided into q equidistant time intervals t_i, such that $\sum_{i=1}^{q} t_i = T$, and $t_i = (\mu_i \pm \delta)$, where μ_i denotes the mean value of t_i and δ represents the relaxation period.

By treating satellite instances as graph nodes and the HO decision-making criteria as directed weighted edges, the timing and target sequence for HOs during the period T are determined by identifying the highest-ranking path in the directed weighted graph. Figure 4 depicts the directed weighted time-based graph representing LEO satellites and base stations. In this graph, straight edges denote transitions between different instances of the same satellite/base station (no HO), while diagonal edges represent HOs between instances of two different satellites/base stations with overlapping coverage periods. The weight of each directed edge is calculated as a weighted summation of decision parameters, collectively forming the HO decision-making criteria.

Figure 5 provides a depiction of a sample graph alongside its real-world counterparts, which are symbolically represented by the graph's elements. Each node within the graph signifies either base stations or satellites. These vertices are, denoted by $V = b_m, s_q$.

The edges within the graph symbolize the times that take to HO from one base station to a satellite. Edge weights represent the time-weighted decision parameters RSS, SNR and elevation angle denoted by M, and the edges itself is represented by $E = x_{gNB}, x_{sat}$ where $x \in M$ encompassing all elements of M. The dotted lines represent the HO between the nodes. This is between either two base stations or between a base station and satellite. Within the scope of this work only HO between the last base station and the satellite is considered. Nevertheless, our proposed strategy possesses the flexibility to accommodate both scenarios by the addition or removal of nodes within the graph.

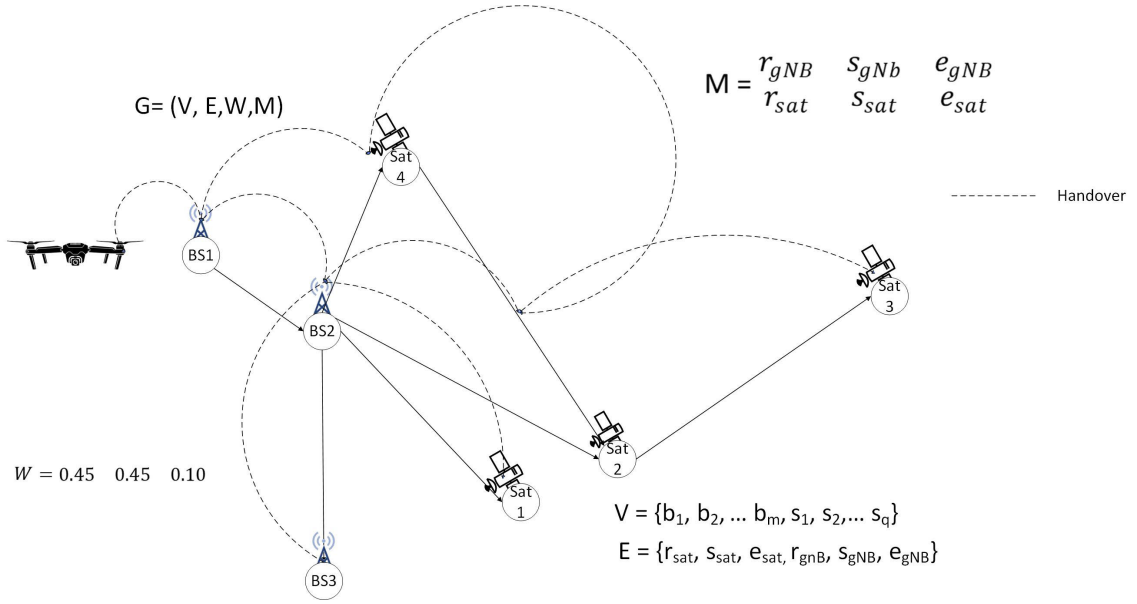

FIGURE 5. Graph representing the possible handovers.

The optimal sequence of HOs within the graph is established through the application of Dijkstra's Algorithm. This algorithm is employed to identify the shortest path between two specified nodes, with the shortest path being defined as the route characterized by the minimal summation of weighted edges.

Thus, the graph is represented as a set of all nodes, edges, weights, and the performance matrix is shown as follows,

$$G = \{V, E, W, M\} \tag{1}$$

where, V is the set of all the nodes, i.e., base stations and satellites.

$$V = \{b_1, b_2 \dots b_m, s_1, s_2 \dots s_q\} \tag{2}$$

E is the set of all decision parameters as defined in (11),

$$E = \{x_{gNB}, x_{sat}\} \tag{3}$$

where, $x \in M$.

C. MODELLING THE DECISION PARAMETERS

In this work, we use RSS as shown in (4), SNR as shown in (10) and elevation angle for the UAV to satellite are considered as decision making signal parameters.

The RSS is the measured received power at UAV i transmitted by base station m. $P_{i,m}$ is considered to be log-normal, thus the random variable $P_{i,m}$ is Gaussian [50]

$$P_{i,m}(dBm) \sim N(\overline{P}_{i,m}(dBm),\ \sigma^2_{dB}) \tag{4}$$

where,

$$\overline{P_{i,m}}(dBm) = \Pi_0(dB) - 10n_p \log_{10}(d_{i,m}/\Delta_0) \tag{5}$$

Here, $\overline{P}_{i,j}(dBm)$ is the mean power in dBm, σ^2_{dB} is the variance of shadowing and Π_0 is calculated from the free space path loss formula [51].

The SNR is calculated as the ratio of signal power and the noise power. Therefore, it is denoted as,

$$SNR = \left|\frac{P_s}{P_N}\right| \tag{6}$$

where, P_s is the signal power and P_N is the noise power.

If the signal is represented as $s(t)$, and it is deterministic then $|P_s|$ is defined to be:

$$P_s = \frac{1}{T}\int_0^T s^2(t)dt \tag{7}$$

where $|T|$ is the observation duration interval. The $|T|$ is equal to the period of $s(t)$ and the root mean square (rms) value equals the square root of its power.

The noise is represented as $|N(t)|$ and has a stochastic description. Thus, the correlation function for noise signal can be written as:

$$R_n(\tau) \equiv E[n(t)n(t+\tau)] \tag{8}$$

Here, $E[\cdot]|$ denotes expected value. P_N is thus related to its correlation function as follows,

$$P_N = |R_n(0)| \tag{9}$$

In this work, however, a white noise system is assumed. This means the correlation function is equal to $|N_0/2 \cdot \delta(t)|$, where $\Delta(t)$ is known as Dirac's delta function [52]. and $N_0/2$ is the spectral height of the white noise and corresponds to the value of noise power spectrum at all frequencies. The SNR

changes to the following,

$$SNR = \left| \frac{\int s^2(t)dt}{N_0/2}. \right| \tag{10}$$

Given below is the performance matrix M, which is a 3×2 matrix, representing the 3 different RF parameters and 2 different networks.

$$M = \begin{bmatrix} r_{gnb} & s_{gnb} & e_{gnb} \\ r_{sat} & s_{sat} & e_{sat} \end{bmatrix} \tag{11}$$

where, $r_{gnb}, s_{gnb}, e_{gnb}$ are the RSS, SNR and elevation angle probabilities associated with the gNB and $r_{sat}, s_{sat}, e_{sat}$ are the RSS, SNR and elevation angle probabilities associated with the satellite.

The decision-making parameters are implemented as a WSM. A WSM is a mathematical framework that combines multiple factors by assigning specific weights to each one. These weights reflect the relative importance or contribution of each factor to an overall outcome. The model computes the result by multiplying each factor by its corresponding weight and then summing these products. This approach allows for customised and flexible analyses, making it valuable in decision-making problems such as UAV-satellite networks, where different signal parameters must be considered with varying degrees of significance to make informed decisions.

For this, we define a weight matrix that assigns weighted probabilities to each parameter. This is written as:

$$W = \begin{bmatrix} 0.45 & 0.45 & 0.10 \end{bmatrix} \tag{12}$$

The last step is to normalise the performance matrix and then add weights to the normalised matrix. If the normalised matrix is represented as v_{ij}, then,

$$v_{ij} = \frac{a_{ij}}{a_j^{max}} \tag{13}$$

and,

$$v_{ij} = \frac{a_j^{min}}{a_{ij}} \tag{14}$$

where, a is an element of (11).

From, above equations, the WSMcan be represented as follows,

$$v_i = \sum_j v_{ij} w_j \tag{15}$$

where, v_{ij} is the normalized performance matrix and w_j is an element.

D. DIJKSTRA'S ALGORITHM

Dijkstra's algorithm is a widely used graph traversal and shortest-path-finding algorithm. It efficiently calculates the shortest path from a source node to all other nodes in a weighted, directed graph. Dijkstra's algorithm starts by initialising distances to all nodes from the source as infinity, except the source itself, which is set to zero. It maintains a set of unvisited nodes and repeatedly selects the node with the smallest distance as the current node. For the current node, it explores its neighbours and updates their distances. If a shorter path is found, the distance to that neighbour is updated. This process continues until all nodes are visited or the target node (if specified) is reached.

Algorithm 1 Dijkstra Algorithm for Shortest Path

Input: No. of nodes and weights of edges
Output: Shortest path to target node

Define the b_{m-1} as the source node in the built graph in the proposed method
Calculate the weight-based cost to each node connected to b_{m-1} as:
$$v_i = \sum_j v_{ij} w_j$$
if $M = r_{gnb}, r_{sat}$ or $s_{gnb} s_{sat}$ **then**
    Mark node with highest v_i
else
    Mark the node with lowest v_i
end if
while s_{m-n} is reached **do**
    Calculate v_i for each node connected to the marked node.
    if $M = r_{gnb}, r_{sat}$ or s_{gnb}, s_{sat} **then**
        Mark node with highest v_i
    else
        Mark the node with lowest v_i
    end if
end while
end

Dijkstra's algorithm uses a priority queue (min-heap) data structure to efficiently select the node with the smallest distance. This data structure ensures that the algorithm runs in O(E + V log V) time complexity, where E is the number of edges and V is the number of vertices in the graph.

E. PROPOSED METHOD

As explained in the previous sections, a graph is built consisting of nodes that are base stations and satellites. The vertices are modelled as a WSM of the decision parameters.

Figure 6, shows the flow diagram for the proposed algorithm. The first step to acquire the measurement reports from the terrestrial base stations and satellites by the UAV. This is fed as input to the algorithm. The RSS, SNR and elevation angle are identified as the decision parameters and their weights analysed. Next, a relaxation period (δ) is selected which is a fraction of the total time period. In graph theory, when finding the shortest path in a graph, relaxation is a fundamental operation. It is used to improve the estimates of the shortest path time periods between vertices. As a time-based graph is considered, shortest path effectively means shortest time taken to transfer control to the node with the best signal parameter, therefore relaxation is referred to as relaxation period. Next, the LEO satellite

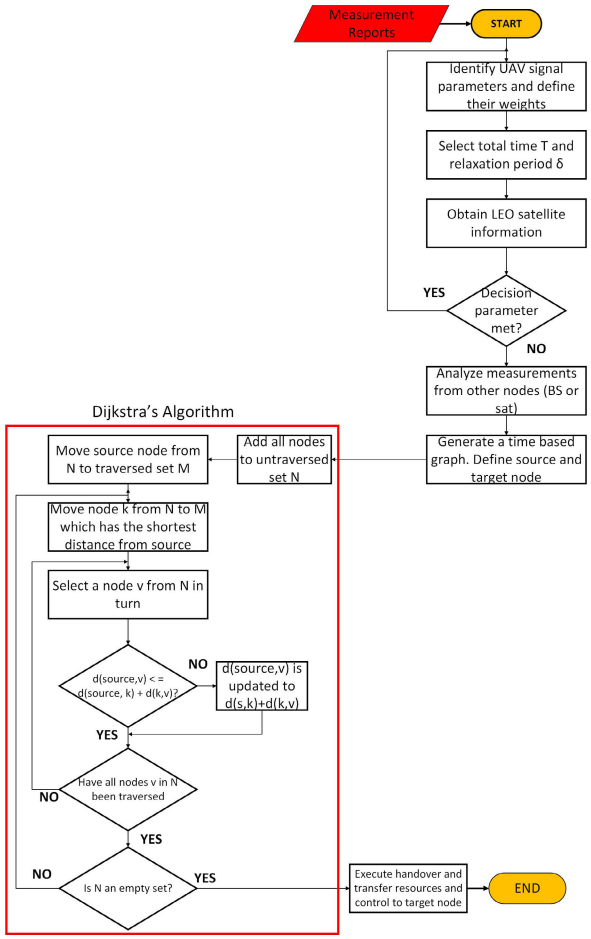

FIGURE 6. Graph-based algorithm flowchart.

information is obtained, in this work we use the Starlink Phase 1 constellation, the data for which is obtained by the work done in [44]. After this, it is checked if the decision parameter of the source node (terrestrial base station in this case) is worse than the destination node (satellite) then HO is performed, else control stays with the source node and the process repeats.

This enables to generate the time-based graph, where then the base station is set as the source and the satellite as the destination and Dijkstra's algorithm is used to find the shortest time period to transfer control to the satellite.

The Dijkstra's algorithm maintains a set of base stations and satellites with tentative time instances from the source. Initially, all nodes except the source gNB have time weights set to infinity, and the source has a time weight of zero. It then repeatedly selects the node with the smallest time period and explores its neighbours to potentially update their times. The following steps briefly explain the process:

- Initialize: Set the time periods of the source node to 0 and all other nodes to infinity. Create a priority queue (or a min-heap) to keep track of the nodes with the smallest tentative time periods.
- Explore Neighbours: While there are nodes in the priority queue, select the node with the smallest tentative time periods. This node is considered visited. For each of its unvisited neighbours, calculate a tentative time period by adding the time periods from the source to the selected node and the edge weight between the selected node and the neighbour. If this tentative time periods are smaller than the current time periods of the neighbour, update the neighbour's time periods.
- Repeat: Continue this process until all nodes have been visited or until the priority queue is empty.
- Shortest Paths: Once the algorithm terminates, you have the shortest time periods from the source node to all other nodes in the graph. These time periods can be used to reconstruct the shortest paths themselves.

Algorithm 2 explains the proposed algorithm in detail. As discussed, previously, the input to the algorithm are the signal parameters and the UAV location. Firstly, the RSS, SNR and elevation angles are defined as the decision parameters. A performance matrix M is defined as the first step to implement the weight summation model. The definition of M is given in (11). The weight matrix is defined as in (12). Next, (11) is normalised to obtain the normalised performance matrix v_i. The time period for the simulation is set as 1800 s and relaxation period δ is set as 300 s.

Algorithm 2 Graph Theory Algorithm for Handover Sequence Selection

Input: UAV location, RSS, SNR, and elevation angle
Output: Optimised handover sequence

1: Define signal performance parameters as decision parameters, RSS, SNR, and elevation angle
2: Define performance matrix M
3: Define weight matrix W
4: Normalize the performance matrix M and obtain normalized performance matrix v_i
5: Select time duration T and relaxation time δ
6: Obtain LEO satellite information
7: Define Appropriate Channel Model

$$G = 20log(c) - 20log(4\pi df) + 10log(A(d)) + \chi$$

8: Select a beginning node b_{m-1} directed to the 1^{st} node (in this case a base station instance)
9: Add a virtual end node s_{m-n} in this case an instance of satellite
10: Solve the graph from first to last node using Algorithm 2 to obtain optimal handover sequence

The next step is to obtain the satellite information for the LEO Starlink Phase 1 constellation. The channel model is defined in the next step, this detailed in further sections. Finally, Dijkstra's algorithm to perform the HO from the source to the target is implemented.

F. HANDOVER STAGES

Performing HO seamlessly involves three main stages: preparation, execution, and completion. These three stages entail various steps that transfers the UAV association from

the base station to a satellite. These stages are shown in figure 7 and explained in detail as follows:

There are 5 elements that enable a seamless HO between the future next generation NodeB (gnB) and satellite in a future 6G network: the UAV, source future gNB, target satellite, the Access and Mobility function (AMF) and the User Plane Function (UPF). The functions of the AMF and UPF are described in [3].

1) Preparation: The first stage of HO involves preparing the different elements to carry out the process. The AMF broadcasts all the mobility related information to every element, while the UAV gets the measurement reports from the source node. The decision parameters: RSS, SNR and elevation angles are analysed for their weights and priority and then the HO decision is made. Once the HO decision is made, then the request is sent to transfer control from the future gNB to the satellite to the AMF. The AMF then, acknowledges the request, and sends the admission control command, enabling the UAV to connect to the satellite.
2) Execution: In this second stage, the execution of the HO takes place, after preparation. The first step is to reconfigure all the Radio Resource Control (RRC) connection, primarily the ''mobilityControlInformation'', which is responsible for carrying all the information is updated. Then the UAV detaches from the old cell and synchronises with the satellite. Any buffered or in-transit packets at this stage is re-routed to the satellite. Next, Sequence Number (SN) status transfer is sent to the AMF by the future gnB, which ensures that the packet data convergence protocol is transferred from the source to the target [53]. The AMF sends the SN status transfer to the satellite. The RRC reconfiguration is completed, and the UAV now synchronises with the satellite. The last step of execution is the UAV requesting the patch switch from the gNB to the satellite.
3) Completion: In this stage, the final steps are performed, and the HO is said to be completed. Firstly, the path switch request is received, the UPF updates its plane to associate with the satellite. The path switch acknowledgement is then sent across to the satellite and the UAV. The last step is to release the context from the gNB, which refers to releasing the resources of the network.

V. SIMULATION SET-UP AND RESULTS

Within the scope of this study, the UAV path involves a transition from an urban environment to a rural area devoid of terrestrial infrastructure, followed by a return to an urban area. Consequently, the HO process encompassing the transition from the final base station to the satellite and subsequently back to the base station is examined.

The evaluation of the HO process unfolds through a dual perspective. First, the examination of variations in decision parameters, specifically RSS and SNR, serving as metrics for evaluating HO performance is studied. Additionally, the evaluation extends to the analysis of QoS parameters, focusing on throughput and latency as indicators of performance.

TABLE 4. 5G parameters.

Parameters	Value
Maximum gNB Power	46 dBm
Antenna Gain	8 dBi
Cellular geometry	Hexagonal
Cell Radius	150m
Frequency	6 GHz
Modulation type	QPSK
Satellite in-view periods (Max, Min)	(750 s @ 10 °) (180 s @ 10 °)

TABLE 5. UAV parameters.

Parameter	Value
UAV altitude	100 m
UAV transmitting power	23 dBm
Average UAV speed	20 m/s
Probability of P_{LoS}	0.8

TABLE 6. Satellite parameters.

Parameter	Value
Elevation angle	10°
Satellite Orbit	550 km
Orbit Inclination	53°
Orbit eccentricity	0 (circular orbit)
Frame of reference	Earth Centred Inertial (ECI)
Transmitting Power	30 dBm

A. SYSTEM MODEL

We consider a three-layer system, as shown in figure 2. The ground segment consists of a 5G gNB, to which the UAV is initially associated with. The gNB and by extension the UAV associated with it is part of the cellular 5G network. We use the sub-6GHz frequency for the gNB, at maximum transmitting power of 5G. The satellite in-view periods lie between the 180 s and 750 s at an elevation angle of 10 °. All the parameters are listed in Table 4 [54].

The air segment consists of the UAV, which is first associated with the gNB and then to the satellite. The proposed algorithm is deployed on-board of this UAV. It flies at a height of 100 m at an average speed of 20 m/s. It uses an omni-directional antenna with a transmitting power of 23 dBm. These parameters are summarized in Table 5

Finally, the space segment consists of the LEO satellite constellation. In this work, the Starlink Phase 1 satellite constellation at 550 km orbit is considered. The UAV sees at a 10 ° elevation angle. These parameters are shown in table 6 [44].

B. NETWORK MODEL

In this work, we consider a scenario of a quasi-stationary fixed cell which does not consist base stations. We assume, the UAV moving with a velocity of v moving out of a cellular network with at least one gNB represented by

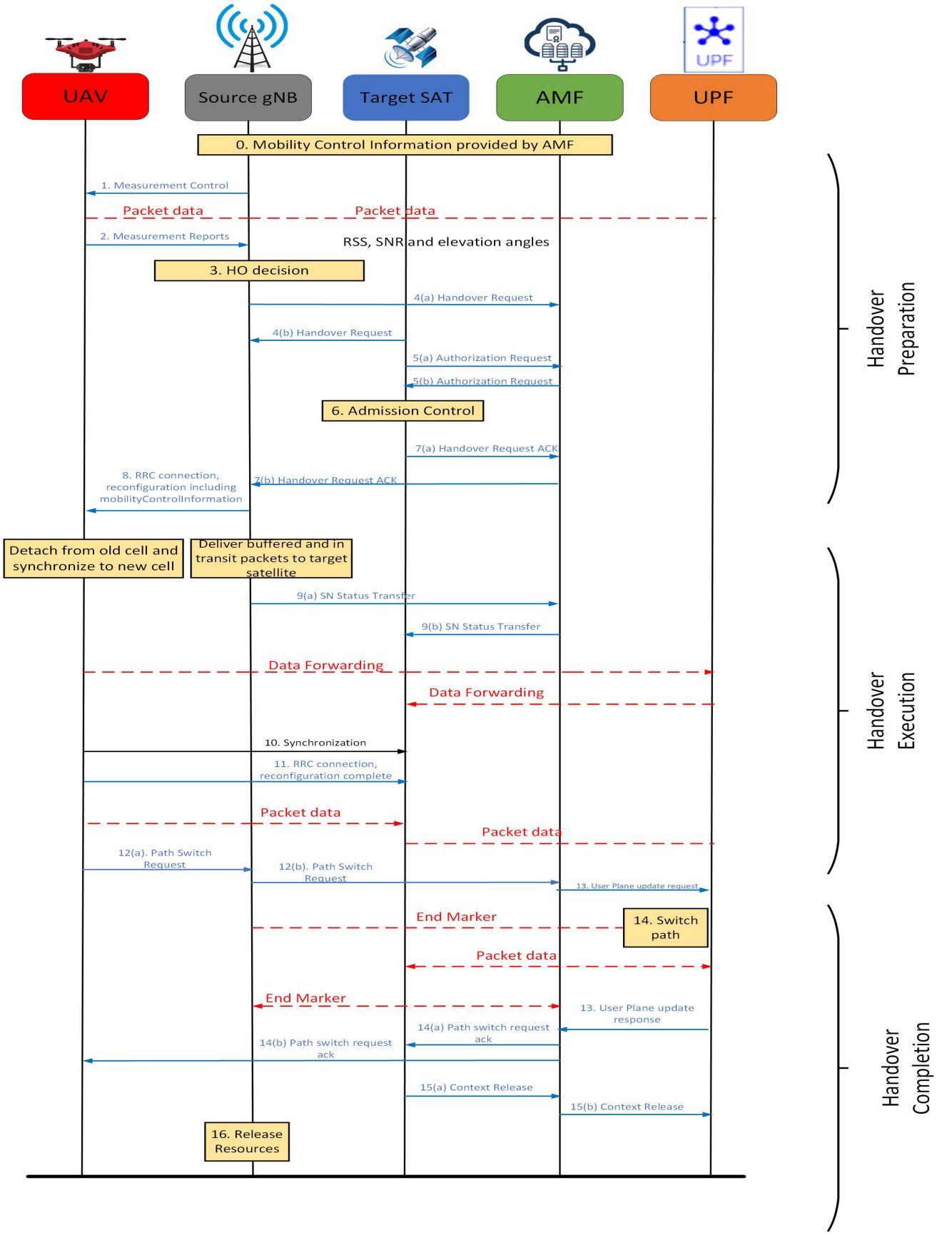

FIGURE 7. Signal flow diagram for stages of handover.

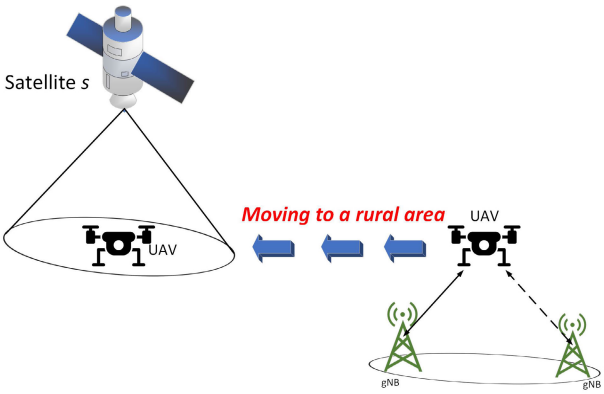

FIGURE 8. Handover scenario.

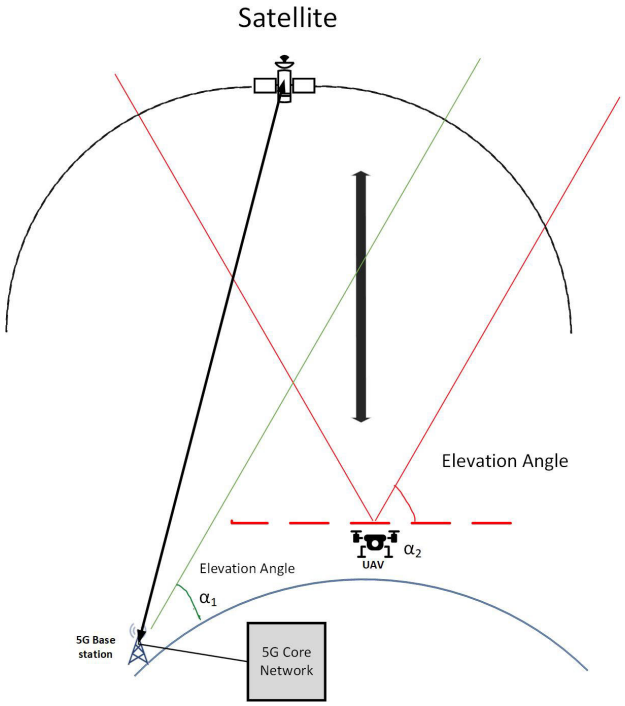

FIGURE 9. System model.

$B = b_1, b_2, \ldots b_m$ into the quasi-stationary cell as shown in figure 8.

This area is covered by satellite represented by $S = s_1, s_2, \ldots s_m$. The satellite is seen by the UAV at an elevation angle of α as shown in figure 9. This complete network is modelled as a graph $G = (n, E)$, where n represents the nodes, i.e., either satellite or gNB and E represents the edges that are the weighted summed functions explained earlier.

C. CHANNEL MODEL

The channel model considers Rician small-scale fading and atmospheric fading [44]. The Rician fading is defined by two parameters. The first one, is the ratio between the power in the direct path and the power in the scattered paths,

$$K = \frac{u^2}{2\beta^2} \tag{16}$$

The second one, is the Ω is the total power from both paths and functions as a scaling factor to the distribution,

$$\Omega = u^2 + 2\beta^2 \tag{17}$$

The amplitude of the signal therefore is Rice distributed with these parameters,

$$u^2 = \frac{K}{1+K}\Omega \tag{18}$$

$$\beta^2 = \frac{\Omega}{2(1+K)} \tag{19}$$

The resulting probability distribution function (φ) is:

$$\varphi = \frac{2(K+1)x}{\Omega} exp\left(-K - \frac{(K+1)x^2}{\Omega}\right) I_0\left(2\sqrt{\frac{K(K+1)}{\Omega}}x\right) \tag{20}$$

The atmospheric fading $A(d)$ is given by.

$$A(d) = 10^{\frac{3d\chi}{10h}} \tag{21}$$

where, χ is the attenuation through the clouds and rain in dB/km, h is the UAV altitude and d is the propagation distance between satellite and the UAV, calculated by,

$$d = \sqrt{h^2 + (x - o_x)^2 + y - o_y^2} \tag{22}$$

where (o_x, o_y) is the position right below the satellite.

Combining 21 and 22, the channel model expression is written as,

$$G = \frac{c}{4\pi d f_c}^2 A(d)\varphi \tag{23}$$

where,

c: Speed of light (3×10^8 m/s)
d: transmission distance (as calculated in (22))
f_c : Operating frequency
$A(d)$: Atmospheric fading (as calculated in (21)
φ : Rician small scale fading (as calculated in (20)

D. RESULTS

In the sections above, we detail the use of the system, channel, and network model for conducting simulations. These simulations have a duration of 1800 seconds (30 minutes) with a relaxation period of 240 seconds.

1) DECISION PARAMETERS

This work employs three decision parameters: RSS, SNR, and elevation angle. The results of these simulations are analysed by plotting these parameters in conjunction with QoS parameters.

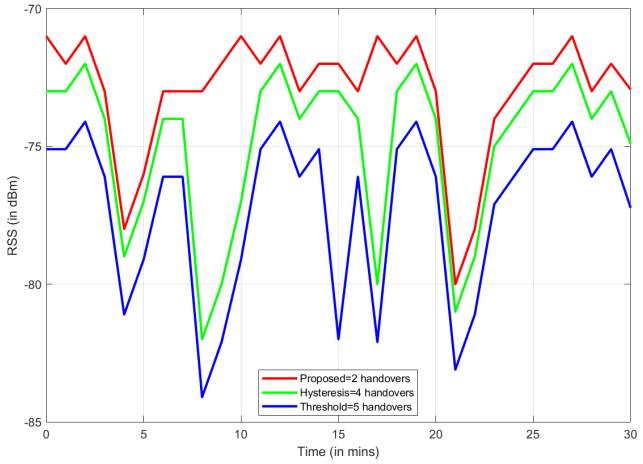

FIGURE 10. RSS vs time.

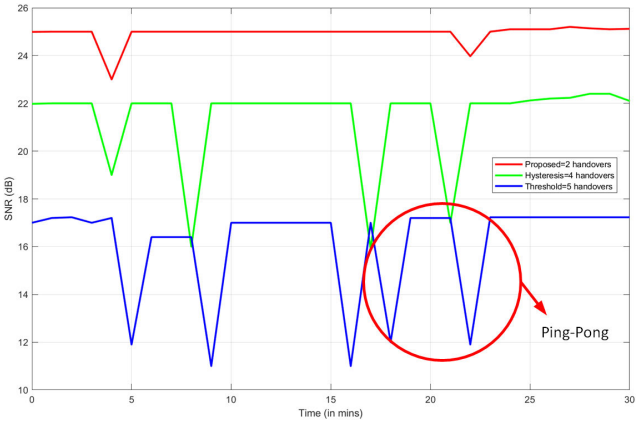

FIGURE 11. SNR vs time.

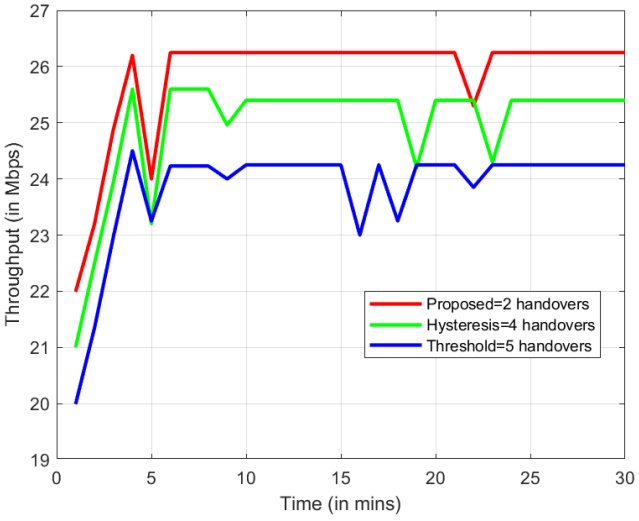

FIGURE 12. Throughput vs time.

- RSS: RSS is a measure of the received radio signal's power by a UAV, reflecting signal strength or intensity. Values typically range from −70 dBm to −90 dBm within the sub-6 GHz spectrum. Variations in RSS over time indicate potential HOs.
- SNR: SNR compares the strength of the desired signal to unwanted noise, determining signal quality and reliability. Higher SNR values indicate better performance, while lower SNR values can lead to connectivity issues.

2) QOS PARAMETERS

Two QoS parameters are analysed to assess the proposed HO algorithm's impact on the communication link:

- Throughput: This measures the data transfer rate over a wireless network, a critical factor for network performance.
- Latency: Latency measures the delay in data transmission, with lower latency being desirable for faster data transfer.

Additionally, the number of ping-pong HOs is measured. Ping-pong HOs refer to situations where a UAV repeatedly switches its connection between two or more base stations. The performance of decision parameters is depicted in Figure 10, which shows RSS plotted against time for three methods: the proposed graph method, hysteresis method, and threshold method.

The graph method shows an average RSS of −72.933 dBm with only 2 HOs, outperforming the other methods. The hysteresis method has an average RSS of −74.9 dBm with 4 HOs, while the threshold method performs the poorest, with over 5 HOs and an average RSS of −77.23 dBm. SNR performance is evident in Figure 11, where the graph method excels with the fewest HOs. The hysteresis method and the threshold method under-perform in both SNR and frequency of HOs. The higher number of HOs is partly due to ping-pong HOs, as indicated in the plot.

QoS parameter analysis is presented in Figure 12, where the implementation of the graph method improves throughput values compared to the other methods. This is attributed to efficient HOs' positive impact on communication system performance. The hysteresis and threshold methods are affected by their drawbacks and the occurrence of ping-pong HOs.

Figure 13 illustrates latency, showing that the implementation of the graph method reduces latency compared to the other methods. Efficient HOs play a crucial role in enhancing communication system performance, while the hysteresis and threshold methods suffer from their drawbacks and the occurrence of ping-pong HOs.

To visualize the HO process better, network status plots are provided for each of the three methods. Figure 14 displays the UAV's network status, indicating connections to the satellite or the 5G network at different time instances. Like the decision parameter plots, HOs occur at 300 s and 1320 s.

In Figure 15, the network status for the hysteresis method is shown, revealing 4 HOs at 300 s, 480 s, 1020 s, and 1320 s.

Lastly, Figure 16 depicts the network status for the UAV using the threshold method, with 5 HOs and one ping-pong HO, occurring at 1020 s and 1260 s.

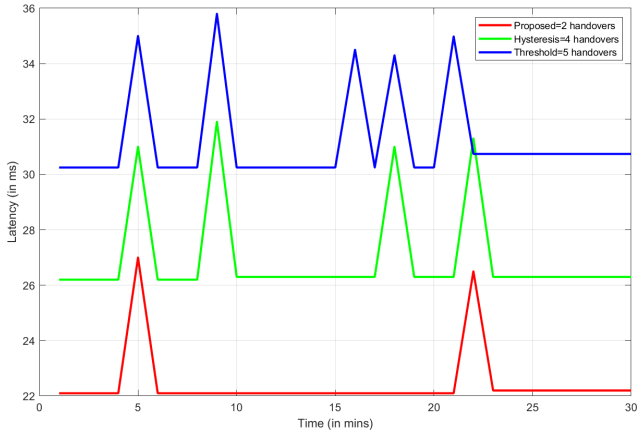

FIGURE 13. Latency vs Time.

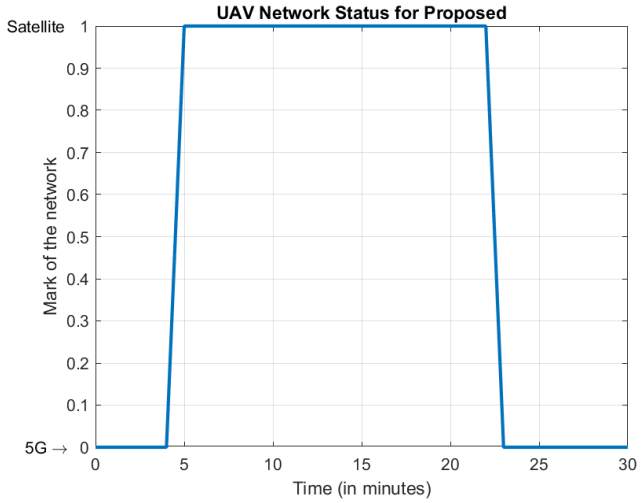

FIGURE 14. Network status for proposed GM.

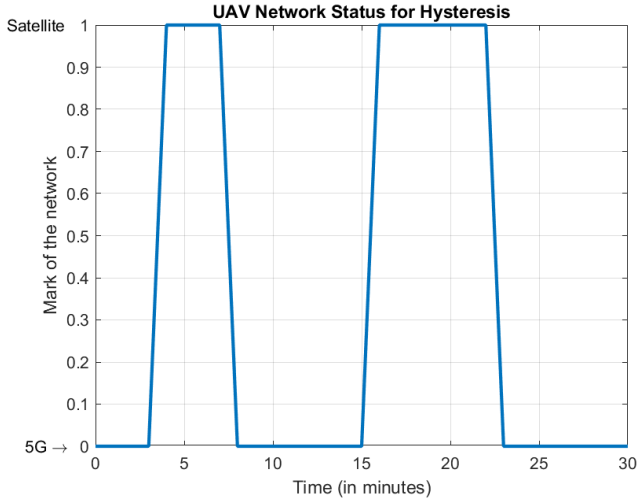

FIGURE 15. Network status for hysteresis method.

These results are obtained with a relaxation period set to 240 s. However, altering this value impacts link performance.

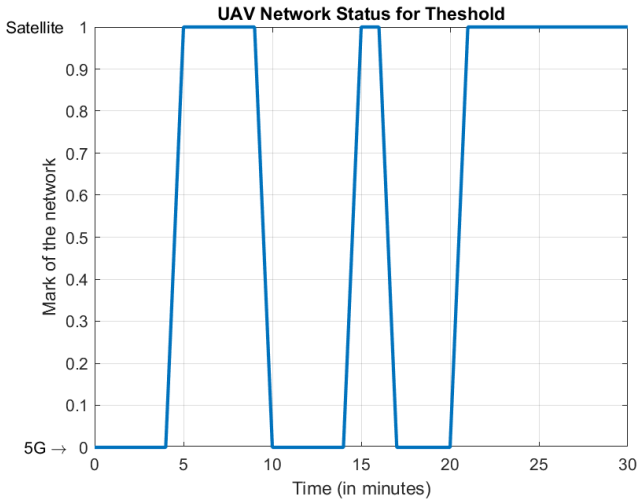

FIGURE 16. Network status for threshold method.

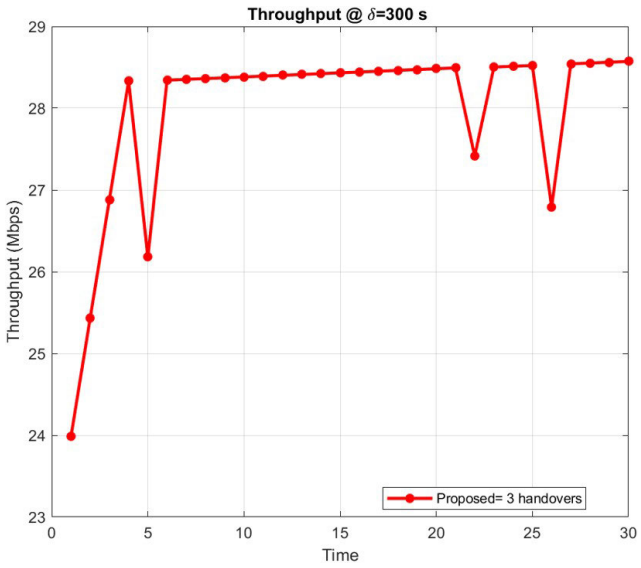

FIGURE 17. Throughput vs time at $\delta = 300$ *s*.

When the relaxation period is set to $\delta = 300$ s, throughput improves by 7.94%, averaging 27.98 Mbps, but an additional HO occurs at 1560 s as shown in figure 17. This is due to Algorithm 1 exploring more nodes in the graph, potentially finding better solutions but also leading to more HOs.

Figure 18 illustrates the latency plot for $\delta = 300$ *s*, reflecting an 8% improvement in values. However, an additional HO is observed, as previously explained.

Increasing the relaxation period to $\delta = 360$ s, as shown in Figure 19, leads to a notable throughput enhancement, with a 16.74% increase compared to $\delta = 240$ s and an 8.14% increase compared to $\delta = 300$ s. HOs occur at 300 s, 1320 s, and 1560 s, similar to the $\delta = 300$ s scenario, with an additional HO at 1200 s.

In Figure 20, the latency plot for $\delta = 360$ *s* reflects an approximate 9.88% improvement in values, similarly accompanied by an additional HO, as previously discussed.

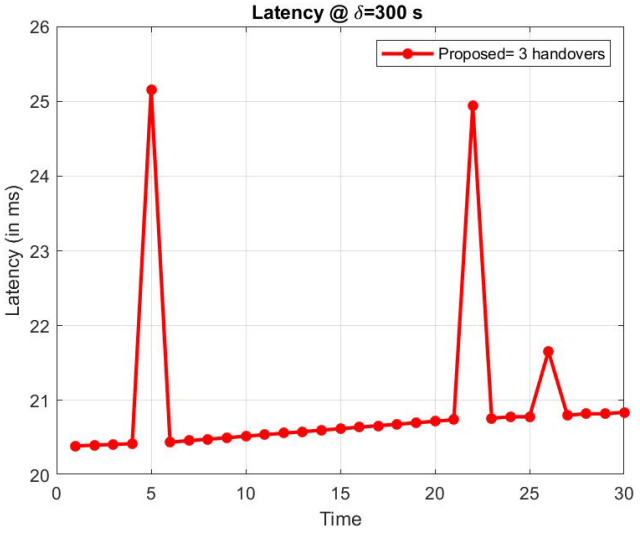

FIGURE 18. Latency vs time at $\delta = 300$ *s*.

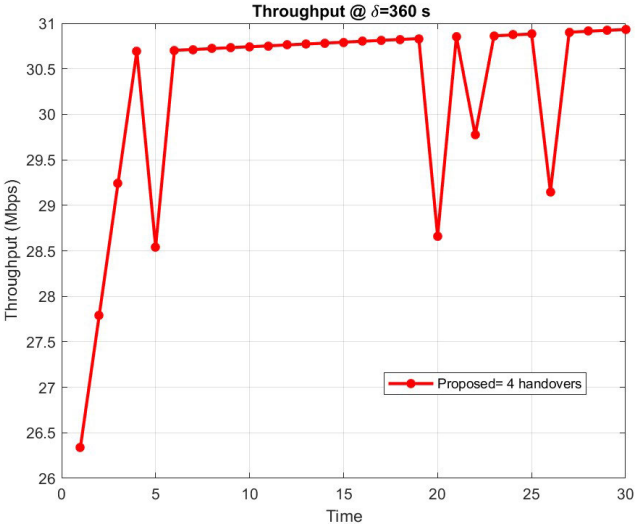

FIGURE 19. Throughput vs time at $\delta = 360$ *s*.

Hence, the choice of relaxation period should consider the UAV's application requirements, as it affects link performance and the frequency of HOs.

To analyse the performance of the algorithms, the number of ping-pongs is measured. In figure 21, it is seen that proposed GM has no ping-pongs while the threshold method has maximum ping pong HOs.

Finally, the probability of which decision parameters is chosen by the WSM model is presented in figure 22

RSS is given the highest weight in the simulation; therefore, it is selected with the highest probability as a decision parameter.

As evident from the aforementioned findings, the devised approach demonstrates superior performance compared to certain prevailing industry benchmarks. Nevertheless, the graph theory algorithm proposed herein is not without its constraints. Notably, in the context of exceptionally extensive networks, the application of the graph method necessitates augmented storage capacities, posing a potential challenge

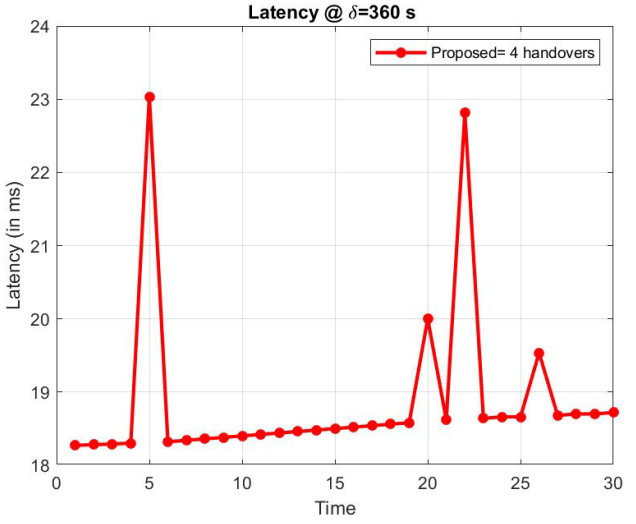

FIGURE 20. Latency vs time at $\delta = 360$ *s*.

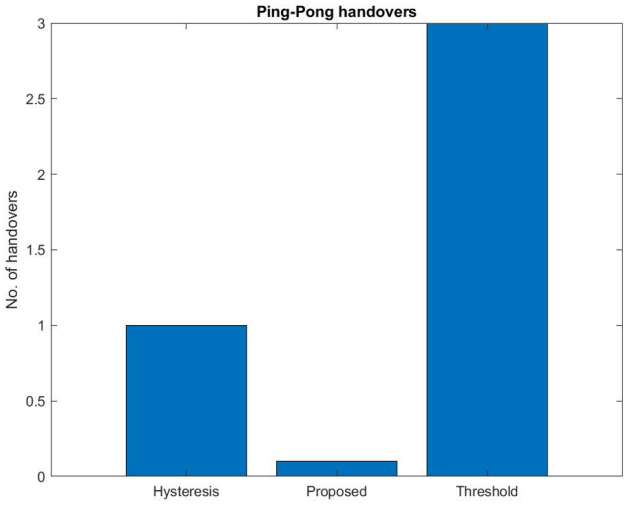

FIGURE 21. No. of Ping-Pongs.

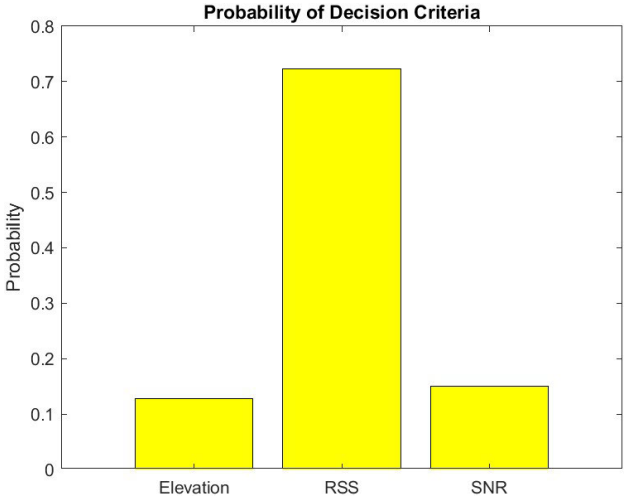

FIGURE 22. Probability of decision parameters.

in deployment scenarios involving UAVs. It is anticipated that forthcoming advancements in storage hardware will

offer a viable resolution to this issue. Additionally. this work does not delve into the satellite visibility problem, working under the assumption that the UAV sees the satellite all the time. However, LEO satellite have a short visibility times ranging from 240 s to 1200 s necessitating satellite to satellite handover, (not part of the scenario considered for this work) which would be a potential next step from this to fully integrate the space based satellite network including GEO satellites.

VI. CONCLUSION

In conclusion, the integration of UAVs into future 6G networks holds great promise for a wide range of applications, from surveillance to precision agriculture and beyond. However, the challenge of ensuring uninterrupted connectivity for UAVs in remote and dynamic environments cannot be overstated. This paper has presented a groundbreaking approach to addressing this challenge by leveraging graph theory and developing a decision-making algorithm for optimizing HOs between terrestrial and satellite communication networks. Through a dynamic network node model, and a decision-making algorithm that considers several factors, such as RSS, SNR and elevation angle, this research has demonstrated a seamless transition between communication links, significantly reducing service disruption. The extensive simulations and comparisons with existing solutions have highlighted substantial improvements in key metrics like RSS, SNR throughput, latency, and ping-pongs, leading to an overall enhancement of UAV connectivity. This graph-based seamless HO solution represents a pivotal advancement in enabling reliable and uninterrupted communication for UAVs operating in remote and challenging environments. By effectively managing HOs between terrestrial and satellite networks, this paper contributes significantly to unlocking the full potential of UAVs in emerging applications, thus pushing the boundaries of UAV technology. As we move forward into the era of 6G networks, this work will play a vital role in shaping the future of UAV technology and its myriad applications.

REFERENCES

[1] X. Liu, H. Zhang, M. Sheng, W. Li, S. Al-Rubaye, and K. Long, "Ultra dense satellite-enabled 6G networks: Resource optimization and interference management," *China Commun.*, vol. 20, no. 10, pp. 1–14, May 2023.

[2] M. Alzenad and H. Yanikomeroglu, "Coverage and rate analysis for vertical heterogeneous networks (VHetNets)," *IEEE Trans. Wireless Commun.*, vol. 18, no. 12, pp. 5643–5657, Dec. 2019.

[3] A. Warrier, S. Al-Rubaye, D. Panagiotakopoulos, G. Inalhan, and A. Tsourdos, "Interference mitigation for 5G-connected UAV using deep Q-learning framework," in *Proc. IEEE/AIAA 41st Digit. Avionics Syst. Conf. (DASC)*, Sep. 2022, pp. 1–8.

[4] M. Ozpolat, S. Al-Rubaye, A. Williamson, and A. Tsourdos, "Integration of unmanned aerial vehicles and LTE: A scenario-dependent analysis," in *Proc. Int. Conf. Connected Vehicle Expo (ICCVE)*, Mar. 2022, pp. 1–6.

[5] S. Mondal, S. Al-Rubaye, and A. Tsourdos, "Handover prediction for aircraft dual connectivity using model predictive control," *IEEE Access*, vol. 9, pp. 44463–44475, 2021.

[6] FC Commission. *SpaceX Non-geostationary Satellite System Attachment a Technical Information to Supplement Schedules*. Accessed: Dec. 3, 2023. [Online]. Available: https://fcc.report/IBFS/SAT-MOD-20181108-00083/1569860

[7] X. Li, H. Zhang, H. Zhou, N. Wang, K. Long, S. Al-Rubaye, and G. K. Karagiannidis, "Multi-agent DRL for resource allocation and cache design in terrestrial-satellite networks," *IEEE Trans. Wireless Commun.*, vol. 22, no. 8, pp. 5031–5042, May 2023.

[8] S. Al-Rubaye, J. Rodriguez, L. Z. Fragonara, P. Theron, and A. Tsourdos, "Unleash narrowband technologies for industrial Internet of Things services," *IEEE Netw.*, vol. 33, no. 4, pp. 16–22, Jul. 2019.

[9] *Study on New Radio (NR) to Support Non Terrestrial Networks*, Standard 38.811, v15.0.0, 3GPP, 2018. [Online]. Available: https://portal.3gpp.org/desktopmodules/Specifications/SpecificationDetails.aspx?specificationId=3234

[10] *Solutions for NR to Support Non-Terrestrial Networks (NTN)*, Standard 38.821, v0.7.0, 3GPP, 2019. [Online]. Available: https://portal.3gpp.org/desktopmodules/Specifications/SpecificationDetails.aspx?specificationId=3525

[11] *Study on Using Satellite Access in 5G. Stage 1*, Standard 38.822, v16.0.0, 3GPP, 2019. [Online]. Available: https://portal.3gpp.org/desktopmodules/Specifications/SpecificationDetails.aspx?specificationId=3372

[12] K. Liolis, A. Geurtz, R. Sperber, D. Schulz, S. Watts, G. Poziopoulou, B. Evans, N. Wang, O. Vidal, B. T. Jou, M. Fitch, S. D. Sendra, P. S. Khodashenas, and N. Chuberre, "Use cases and scenarios of 5G integrated satellite-terrestrial networks for enhanced mobile broadband: The SaT5G approach," *Int. J. Satell. Commun. Netw.*, vol. 37, no. 2, pp. 91–112, Mar. 2019.

[13] C. Ge, N. Wang, I. Selinis, J. Cahill, M. Kavanagh, K. Liolis, C. Politis, J. Nunes, B. Evans, Y. Rahulan, N. Nouvel, M. Boutin, J. Desmauts, F. Arnal, S. Watts, and G. Poziopoulou, "QoE-assured live streaming via satellite backhaul in 5G networks," *IEEE Trans. Broadcast.*, vol. 65, no. 2, pp. 381–391, Jun. 2019.

[14] (2019). *Drones in the 5G Era*. [Online]. Available: https://5gdrones.eu/

[15] N. Hosseini, H. Jamal, J. Haque, T. Magesacher, and D. W. Matolak, "UAV command and control, navigation and surveillance: A review of potential 5G and satellite systems," in *Proc. IEEE Aerosp. Conf.*, 2019, pp. 1–10.

[16] I. Shayea, P. Dushi, M. Banafaa, R. A. Rashid, S. Ali, M. A. Sarijari, Y. I. Daradkeh, and H. Mohamad, "Handover management for drones in future mobile networks—A survey," *Sensors*, vol. 22, no. 17, p. 6424, Aug. 2022. [Online]. Available: https://www.mdpi.com/1424-8220/22/17/6424

[17] B. Deebak and F. Al-Turjman, "Drone of IoT in 6G wireless communications: Technology, challenges, and future aspects," in *Unmanned Aerial Vehicles in Smart Cities*. Singapore: Springer, 2020, pp. 153–165.

[18] S. Nayak and R. Patgiri, "6G communication: A vision on the potential applications," in *Proc. 26th Int. Conf. ADCOM*. Cham, Switzerland: Springer, 2022, pp. 203–218.

[19] S. Alraih, I. Shayea, M. Behjati, R. Nordin, N. F. Abdullah, A. Abu-Samah, and D. Nandi, "Revolution or evolution? Technical requirements and considerations towards 6G mobile communications," *Sensors*, vol. 22, no. 3, p. 762, Jan. 2022.

[20] Y. Sun, J. Liu, J. Wang, Y. Cao, and N. Kato, "When machine learning meets privacy in 6G: A survey," *IEEE Commun. Surveys Tuts.*, vol. 22, no. 4, pp. 2694–2724, 4th Quart., 2020.

[21] R. Shafin, L. Liu, V. Chandrasekhar, H. Chen, J. Reed, and J. C. Zhang, "Artificial intelligence-enabled cellular networks: A critical path to beyond-5G and 6G," *IEEE Wireless Commun.*, vol. 27, no. 2, pp. 212–217, Apr. 2020.

[22] Y.-C. Liang, D. Niyato, E. G. Larsson, and P. Popovski, "Guest editorial: 6G mobile networks: Emerging technologies and applications," *China Commun.*, vol. 17, no. 9, pp. 90–91, Sep. 2020.

[23] G. Geraci, D. López-Pérez, M. Benzaghta, and S. Chatzinotas, "Integrating terrestrial and non-terrestrial networks: 3D opportunities and challenges," *IEEE Commun. Mag.*, vol. 61, no. 4, pp. 42–48, Apr. 2023.

[24] N. Kato, B. Mao, F. Tang, Y. Kawamoto, and J. Liu, "Ten challenges in advancing machine learning technologies toward 6G," *IEEE Wireless Commun.*, vol. 27, no. 3, pp. 96–103, Jun. 2020.

[25] B. Zong, C. Fan, X. Wang, X. Duan, B. Wang, and J. Wang, "6G technologies: Key drivers, core requirements, system architectures, and enabling technologies," *IEEE Veh. Technol. Mag.*, vol. 14, no. 3, pp. 18–27, Sep. 2019.

[26] S. Kota and G. Giambene, "6G integrated non-terrestrial networks: Emerging technologies and challenges," in *Proc. IEEE Int. Conf. Commun. Workshops (ICC Workshops)*, Jun. 2021, pp. 1–6.

[27] M. Mozaffari, X. Lin, and S. Hayes, "Toward 6G with connected sky: UAVs and beyond," *IEEE Commun. Mag.*, vol. 59, no. 12, pp. 74–80, Dec. 2021.

[28] Y. Wu, G. Hu, F. Jin, and J. Zu, "A satellite handover strategy based on the potential game in LEO satellite networks," *IEEE Access*, vol. 7, pp. 133641–133652, 2019.

[29] Y. Li, W. Zhou, and S. Zhou, "Forecast based handover in an extensible multi-layer LEO mobile satellite system," *IEEE Access*, vol. 8, pp. 42768–42783, 2020.

[30] J. Li, K. Xue, J. Liu, and Y. Zhang, "A user-centric handover scheme for ultra-dense LEO satellite networks," *IEEE Wireless Commun. Lett.*, vol. 9, no. 11, pp. 1904–1908, Nov. 2020.

[31] Y. Cao, S.-Y. Lien, and Y.-C. Liang, "Deep reinforcement learning for multi-user access control in non-terrestrial networks," *IEEE Trans. Commun.*, vol. 69, no. 3, pp. 1605–1619, Mar. 2021.

[32] Q. Zhang, L. Zhang, Y.-C. Liang, and P.-Y. Kam, "Backscatter-NOMA: A symbiotic system of cellular and Internet-of-Things networks," *IEEE Access*, vol. 7, pp. 20000–20013, 2019.

[33] S. Al-Rubaye and A. Tsourdos, "Connectivity for air mobility transportation in future networks," *IEEE Future Netw. Tech Focus*, vol. 12, no. 12, Apr. 2021.

[34] H. A. Mahmoud, I. Güvenç, and F. Watanabe, "Performance of open access femtocell networks with different cell-selection methods," in *Proc. IEEE 71st Veh. Technol. Conf.*, May 2010, pp. 1–5.

[35] Z. Wang, L. Li, Y. Xu, H. Tian, and S. Cui, "Handover control in wireless systems via asynchronous multiuser deep reinforcement learning," *IEEE Internet Things J.*, vol. 5, no. 6, pp. 4296–4307, Dec. 2018.

[36] A. A. Adewale, E. E. Ekong, F. A. Ibikunle, A. Orimogunje, and J. Abolade, "Ping-pong reduction for handover process using adaptive hysteresis margin: A methodological approach," *IOP Conf. Ser., Mater. Sci. Eng.*, vol. 640, no. 1, Nov. 2019, Art. no. 012118, doi: 10.1088/1757-899x/640/1/012118.

[37] K. Li, Y. Li, Z. Qiu, Q. Wang, J. Lu, and W. Zhou, "Handover procedure design and performance optimization strategy in LEO-HAP system," in *Proc. 11th Int. Conf. Wireless Commun. Signal Process. (WCSP)*, Oct. 2019, pp. 1–7.

[38] S.-Y. Ni, S. Jin, and H.-L. Hong, "A handover decision algorithm with an adaptive threshold applied in HAPS communication system," in *Theory, Methodology, Tools and Applications for Modeling and Simulation of Complex Systems*. Singapore: Springer, 2016, pp. 38–47.

[39] Z. Jia, Q. Wu, C. Dong, C. Yuen, and Z. Han, "Hierarchical aerial computing for Internet of Things via cooperation of HAPs and UAVs," *IEEE Internet Things J.*, vol. 10, no. 7, pp. 5676–5688, Apr. 2023.

[40] F. Hsieh, F. Jardel, E. Visotsky, F. Vook, A. Ghosh, and B. Picha, "UAV-based multi-cell HAPS communication: System design and performance evaluation," in *Proc. GLOBECOM IEEE Global Commun. Conf.*, Dec. 2020, pp. 1–6.

[41] E. De Santis, A. Giuseppi, A. Pietrabissa, M. Capponi, and F. Delli Priscoli, "Satellite integration into 5G: Deep reinforcement learning for network selection," *Mach. Intell. Res.*, vol. 19, no. 2, pp. 127–137, Apr. 2022.

[42] E. Juan, M. Lauridsen, J. Wigard, and P. Mogensen, "Handover solutions for 5G low-Earth orbit satellite networks," *IEEE Access*, vol. 10, pp. 93309–93325, 2022.

[43] L. Zhang, S. Wu, X. Lv, and J. Jiao, "A two-step handover strategy for GEO/LEO heterogeneous satellite networks based on multi-attribute decision making," *Electronics*, vol. 11, no. 5, p. 795, Mar. 2022. [Online]. Available: https://www.mdpi.com/2079-9292/11/5/795

[44] M. Hozayen, T. Darwish, G. K. Kurt, and H. Yanikomeroglu, "A graph-based customizable handover framework for LEO satellite networks," in *Proc. IEEE Globecom Workshops (GC Wkshps)*, Dec. 2022, pp. 868–873.

[45] Y. Zeng, J. Lyu, and R. Zhang, "Cellular-connected UAV: Potential, challenges, and promising technologies," *IEEE Wireless Commun.*, vol. 26, no. 1, pp. 120–127, Feb. 2019.

[46] A. Azari, F. Ghavimi, M. Ozger, R. Jantti, and C. Cavdar, "Machine learning assisted handover and resource management for cellular connected drones," in *Proc. IEEE 91st Veh. Technol. Conf. (VTC-Spring)*, May 2020, pp. 1–7.

[47] A. S. Warrier, S. Al-Rubaye, D. Panagiotakopoulos, G. Inalhan, and A. Tsourdos, "Seamless handover in urban 5G-UAV systems using entropy weighted method," *Int. J. Inf. Commun. Eng.*, vol. 16, no. 9, pp. 373–378, Dec. 2022. [Online]. Available: https://publications.waset.org/vol/189

[48] D. Vallado, P. Crawford, R. Hujsak, and T. S. Kelso, "Revisiting spacetrack report #3," in *Proc. AIAA/AAS Astrodynamics Specialist Conf. Exhibit*, Aug. 2006, p. 6753.

[49] I. Ali, N. Al-Dhahir, and J. E. Hershey, "Predicting the visibility of LEO satellites," *IEEE Trans. Aerosp. Electron. Syst.*, vol. 35, no. 4, pp. 1183–1190, Jun. 1999.

[50] N. Patwari and A. O. Hero, "Using proximity and quantized RSS for sensor localization in wireless networks," in *Proc. 2nd ACM Int. Conf. Wireless Sensor Netw. Appl.*, Sep. 2003, pp. 20–29.

[51] T. Rappaport, *Wireless Communications: Principles and Practice*, 2nd ed. Upper Saddle River, NJ, USA: Prentice-Hall, 1996. [Online]. Available: https://books.google.co.uk/books?id=gPK0DwAAQBAJ

[52] B. Engquist, A.-K. Tornberg, and R. Tsai, "Discretization of dirac delta functions in level set methods," *J. Comput. Phys.*, vol. 207, no. 1, pp. 28–51, Jul. 2005. [Online]. Available: https://www.sciencedirect.com/science/article/pii/S002199910500015X

[53] ETSI. (2013). *TS 136 423—v11.5.0—Evolved Universal Terrestrial Radio Access Network (E-UTRAN); X2 Application Protocol (X2AP) (3GPP TS 36.423 Version 11.5.0 Release 11)*. [Online]. Available: http://portal.etsi.org/chaircor/ETSI_support.asp

[54] B. Mondal, T. A. Thomas, E. Visotsky, F. W. Vook, A. Ghosh, Y.-H. Nam, Y. Li, J. Zhang, M. Zhang, Q. Luo, Y. Kakishima, and K. Kitao, "3D channel model in 3GPP," *IEEE Commun. Mag.*, vol. 53, no. 3, pp. 16–23, Mar. 2015.

ANIRUDH WARRIER received the degree in electronics and communications engineering from the SRM Institute of Science and Technology, India, and the master's degree in astronautics and space engineering from Cranfield University, in September 2019. He is currently pursuing the Ph.D. degree, researching to developing air to ground connectivity for 5G UAV networks, under Prof. Saba Al-Rubaye. He completed the degree thesis in association with the Indian Space Research Organization (ISRO) in 2019. He also completed the master's degree thesis on "Urban Air Mobility Based on Satellite and 5G Communications" under the supervision of Prof. Saba Al Rubaye, in 2020.

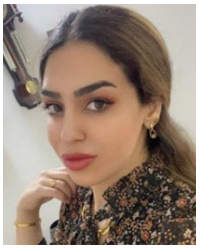

LAMEES ALJABURI is currently pursuing the master's degree in computer engineering with Near East University, Cyprus, which reflects her commitment to furthering her education and research to focus on AI, ML, 6G communications, and networking. She is a dedicated professional with a strong background in computer and communications engineering, with five years of valuable industrial experience.

HUW WHITWORTH received the degree in electronic and communications engineering, with a focus on embedded systems engineering and antenna design from the University of Kent, in Summer 2019, and the M.Sc. degree in applied artificial intelligence from Cranfield University, in September 2019. He is currently pursuing the Ph.D. degree, researching future communication methods and security, under Prof. Saba Al-Rubaye. His M.Sc. thesis was on synthetic data generation for augmenting datasets. He is currently funded by Thales (U.K.) and U.K. DfT, based at Cranfield University's DARTeC Facility, where his research area is future communications networks. His current work includes reviewing data exchanges between actors, analyzing security and vulnerabilities in these networks, and producing countermeasures and security methodologies to existing and zero day cyber threats.

SABA AL-RUBAYE (Life Senior Member, IEEE) is a Professor Chair of telecommunications and autonomous systems with the Centre for Autonomous and Cyberphysical Systems, School of Aerospace, Transport and Manufacturing, Cranfield University, U.K. She is leading and was involved with several projects, including Rise Project, UAS Authentication Service and Aviation Innovation in the South-West, H2020 SESAR AMULED, and DfT–Smart Airport to develop, design new connectivity techniques, and integrated software/hardware hub proof of concept. She is participating in developing industry standards by being an active research group member of IEEE P1932.1 Standard of License/Unlicensed Interoperability and IEEE P1920.2 Standard for Vehicle-to-Vehicle Communications for Unmanned Aircraft Systems. She has published many papers in IEEE journals and conferences. She has delivered tutorials at IEEE ICC, IEEE WCNC, and IEEE VTC conferences; and invited talks at various venues, including the Communications Research Centre (CRC) of Canada, IEEE Toronto Chapter, and IEEE U.K. Chapter. She was a recipient of the Best Technical Paper Award (twice) published in IEEE Vehicular Technology, in 2011 and 2015, respectively. She has been the general co-chair and the TPC co-chair and has held other leading roles of many international conferences. She is a Chartered Engineer (C.Eng.) and a member of the Institute of Engineering and Technology (IET). She is holding commercial certificate of unmanned aircraft systems (UAS) pilot in the U.K.

ANTONIOS TSOURDOS received the M.Eng. degree in electronic, control and systems engineering from The University of Sheffield, in 1995, the M.Sc. degree in systems engineering from Cardiff University, in 1996, and the Ph.D. degree in nonlinear robust autopilot design and analysis from Cranfield University, in 1999. He is the Head of the Autonomous and Cyberphysical Systems Centre and the Centre for Autonomous and Cyberphysical Systems. In 1999, he joined Cranfield University, as a Lecturer. He was appointed as the Head of the Centre for Autonomous and Cyber-Physical Systems in 2007, a Professor of autonomous systems and control in 2009, and the Director of Research–aerospace, transport and manufacturing in 2015. He was a member of Team Stellar, the winning team for the U.K. Ministry of Defence Grand Challenge, in 2008, and an IET Innovation Award, in 2009 (Team category). He is the Chair of the International Federation of Automatic Control (IFAC) Technical Committee on Aerospace Control; and a member of the American Institute of Aeronautics and Astronautics (AIAA), Unmanned Systems Integration and Outreach Committee, the Institute of Electrical and Electronics Engineers (IEEE) Control System Society, the Technical Committee on Aerospace Control (TCAC), and the IMechE Mechatronics, Informatics and Control Group Board. He is an Editorial Board Member of *Proceedings of the IMechE, Part G*, *Journal of Aerospace Engineering*, IEEE TRANSACTIONS ON AEROSPACE AND ELECTRONIC SYSTEMS, *Aerospace Science and Technology*, *International Journal of Systems Science and Control Engineering*, and *International Journal of Aeronautical and Space Sciences*.

https://dspace.org/

Future 6G communications powering vertical handover in non-terrestrial networks

Warrier, Anirudh; Aljaburi, Lamees; Whitworth, Huw; Al-Rubaye, Saba; Tsourdos, Antonios

2024-02-01
Institute of Electrical and Electronics Engineers (IEEE)
https://doi.org/10.1109/ACCESS.2024.3371906
Warrier A, Aljaburi L, Whitworth H, et al., (2024) Future 6G communications powering vertical handover in non-terrestrial networks. IEEE Access, Volume 12, February 2024, pp. 33016-33034

Downloaded from a DSpace repository. https://dspace.org/